

A Crystallographic Study of a Highly Substituted Imidazolinone, (3*S*,4*S*,5*R*)-3-(((*S*)-4-((1*H*-Indol-3-yl)Methyl)-5-Oxo-4,5-Dihydro-1*H*-Imidazol-2-yl)Amino)-4-((*Tert*-Butyldimethylsilyl)Oxy)-5-Hydroxypiperidin-2-One

Sanjay Dutta · Sergey M. Dibrov · Cody J. Higginson · Thomas Hermann

Received: 6 April 2011 / Accepted: 28 May 2011 / Published online: 9 June 2011
© Springer Science+Business Media, LLC 2011

Abstract The title compound **1** has been prepared from the condensation product of a silyl protected amino-oxazoline lactam (**3**) and Cbz-protected *L*-tryptophan (**4**) after hydrogenolysis of the carboxybenzyl protection group. The synthesis and crystal structure of **1** is described. The compound crystallized from DMSO in the monoclinic system, $P2_1$ space group with unit cell parameters $a = 9.4029(25)$, $b = 6.2828(12)$, $c = 20.681(45)$, and $\beta = 96.505(16)$, $Z = 2$ and a cell volume of $V = 1213.9(2) \text{ \AA}^3$. In the crystal lattice, **1** forms an extensive hydrogen bonded framework consisting of interconnected dimeric chains.

Keywords Streptolidine · Imidazolinone · Hydrogen bonding

Introduction

The amino-oxazoline lactam (**2**) is an oxygen analog of the amino acid lactam streptolidine which occurs in natural peptide antibiotics (Fig. 1) [1, 2]. Drug-like properties of the natural products suffer from the guanidinium moiety in the streptolidine scaffold which is positively charged under physiological conditions. We have proposed the amino-oxazole **2** as a less basic structural analog of the streptolidine lactam.

Coupling of silyl-protected **2** with carboxylic acids has been used to prepare compounds that are biased for binding

of structured ribonucleic acid (RNA) targets. When *tert*-butyldimethylsilyl-protected **3** was treated with α -amino Cbz-protected *L*-tryptophan (**4**) under standard peptide coupling conditions the intermediate **5** was obtained (Fig. 2). Hydrogenolysis to remove the Cbz group furnished the highly substituted imidazolinone **1** as a major product which was formed from **6** through intramolecular nucleophilic attack of the α -amino group at the electrophilic carbon center of the oxazoline. While the nucleophilic ring opening of 2-oxazolines is an extensively studied transformation [3], in our system, the intramolecular nature of the reaction leads to the formation of another cyclic system, the imidazolinone **1**. Here, we report the crystal structure of **1**, (3*S*,4*S*,5*R*)-3-(((*S*)-4-((1*H*-indol-3-yl)methyl)-5-oxo-4,5-dihydro-1*H*-imidazol-2-yl)amino)-4-((*tert*-butyldimethylsilyl)oxy)-5-hydroxypiperidin-2-one.

Experimental Section

Commercial reagents were used without any further purification. Anhydrous methanol was purchased from AcroSeal. ^1H NMR and ^{13}C NMR spectra were recorded on a Jeol ECA 500 MHz NMR or a Varian 400 MHz spectrometer. Mass spectra were obtained on a ThermoFinnigan LCQDECA-MS spectrometer.

Benzyl ((*S*)-1-(((3*aS*,7*R*,7*aS*)-7-((*Tert*-Butyldimethylsilyl)Oxy)-4-Oxo-3*a*,4,5,6,7,7*a*-Hexahydro-Oxazolo[4,5-*c*]Pyridin-2-yl)Amino)-3-(1*H*-Indol-3-yl)-1-Oxopropan-2-yl)Carbamate (**5**)

The TBDMS-protected amino-oxazoline core (**3**) was obtained as previously described [4] and coupled to carboxybenzyl-protected *L*-tryptophan (*Z*-Trp-OH) using

Sanjay Dutta, Sergey M. Dibrov contributed equally to this work.

S. Dutta · S. M. Dibrov · C. J. Higginson · T. Hermann (✉)
Department of Chemistry and Biochemistry, University
of California, San Diego, 9500 Gilman Drive, La Jolla,
CA 92093, USA
e-mail: tch@ucsd.edu

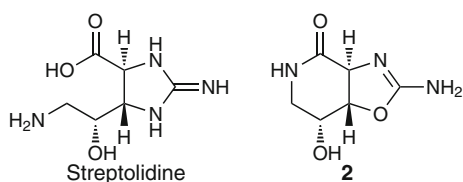


Fig. 1 Structures of the amino acid streptolidine, a constituent of natural peptide antibiotics, and the amino-oxazoline lactam analog **2**

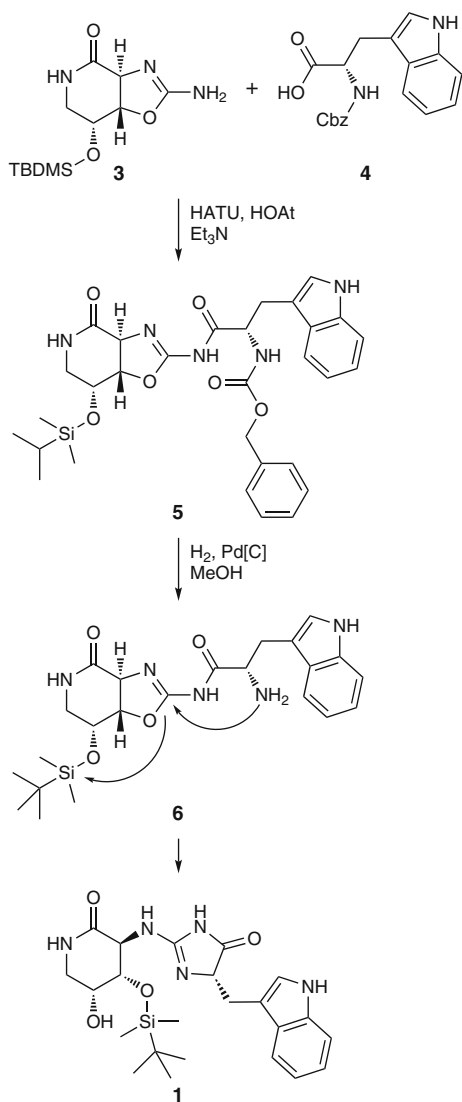


Fig. 2 Synthesis of the title compound **1**

coupling reagents HATU and HOAt (2 eq each), triethylamine (5 eq). Z-Trp-OH (0.62 mmol, 211 mg) was dissolved in 3.7 mL DMF in a dried flask. To the solution was added HATU (0.83 mmol, 170 mg, 2 eq) and HOAt (112 mg, 0.83 mmol, 2 eq) and Triethylamine (5 eq, 2.05 mmol, 275 μ L). Then **3** (0.41 mmol, 118 mg) dissolved in 5 mL DMF was added. The reaction mixture was

heated to 40 °C with stirring for 24 h. After completion of the reaction, 20 mL of water was added and the mixture was extracted with 3 \times 25 mL of chloroform which was washed with equal volumes of 0.1 N HCl and saturated NaHCO₃, then dried over Na₂SO₄. The crude extract was purified by silica column chromatography and applying a solvent gradient beginning with hexane, proceeding through 5% methanol over ethyl acetate. An overall 97% yield of product **5** was obtained after purification. **5**: ¹H NMR (500 MHz, CDCl₃) δ 7.55 (d, 1H), 7.28 (5H), 7.24 (d, 1H), 7.09 (t, 1H), 7.03 (t, 1H), 6.88 (s, 1H), 6.66 (broad, 1H), 5.12 (t, 1H), 5.01 (d, 1H), 4.66 (m, 1H), 3.99 (s, 1H), 3.77 (s, 1H), 3.72 (s, 1H), 3.38 (m, 2H), 3.18 (m, 1H), 0.94 (s, 9H), 0.1 (d, 6H); ¹³C NMR (500 MHz, CDCl₃) δ 168.4, 166.2, 156.4, 156.2, 136.7, 136.2, 128.7, 128.3, 124.1, 121.9, 119.5, 118.8, 111.6, 109.9, 79.6, 66.9, 62.5, 58.9, 50.1, 38.8, 27.9, 25.9, 18.2, -4.6; MS exact mass calculated for C₃₁H₃₉N₅O₆Si 605.27, found 606.27 (M + H)⁺.

(3S,4S,5R)-3-(((S)-4-((1H-Indol-3-yl)Methyl)-5-Oxo-4,5-Dihydro-1H-Imidazol-2-yl)Amino)-4-((Tert-Butyldimethylsilyl)Oxy)-5-Hydroxypiperidin-2-One (**1**)

Compound **5** (240 mg, 0.4 mmol) was dissolved in anhydrous methanol (7 mL) to 0.06 M. 8–12 mol.% Pd of 10% (wt) activated palladium on carbon (24 mg) was added to an oven-dried two-necked round-bottom flask. The flask was purged twice with argon, followed by addition of the **5** solution via a syringe. The flask was then thoroughly purged with hydrogen gas and stirring was started. The progress of the reaction was monitored via TLC (10% methanol in ethyl acetate). After 24 h the reaction mixture was vacuum filtered through Celite followed by washing with methanol. The collected filtrate was condensed. A mixture of compounds **6** and **1** was purified via normal phase silica gel column chromatography and by applying a solvent gradient starting with hexanes and proceeding through 15% methanol in ethyl acetate. The mixture of compounds **6** and **1** was dissolved in methanol and added slowly to a solution of two equivalents of potassium fluoride in methanol, on ice, with stirring. After 1 h, the ice bath was removed and the reaction mixture was allowed to reach room temperature. After standing overnight a white precipitate had formed. Filtration through a sintered funnel and drying gave the precipitated product **1** as a white solid in 65% yield. **1**: ¹H NMR (500 MHz, DMSO) δ 10.9 (s, 1H), 7.9 (s, 1H), 7.58 (t, 1H), 7.48 (t, 1H), 7.33 (td, 1H), 7.20 (dd, 1H), 7.03 (t, 1H), 6.93 (t, 1H), 5.52 (s, 1H, NH), 5.08 (s, 1H), 4.03 (s, 1H), 3.98 (dd, 1H), 3.91 (d, 1H), 3.2 (dd, 1H), 3.10 (dt, 1H), 3.0 (m, 1H), 2.85 (s, 1H), 2.68 (s, 1H), 2.54 (d, 1H), 0.8 (s, 9H), 0.06 (d, 3H), -0.05 (d, 3H).

X-Ray Crystallography

X-ray diffraction data of the title compound were collected on a Bruker Kappa diffractometer equipped with an APEX CCD II area detector using graphite-monochromated Cu K α radiation ($\lambda = 1.54178 \text{ \AA}$). A colorless plate ($0.02 \times 0.10 \times 0.50 \text{ mm}$) was mounted on a cryoloop with paratone oil. Data were collected in a nitrogen gas stream at 173(2) K using φ and ω scans. The data were integrated using the Bruker SAINT [5] software and scaled using the SADABS [6] program. Solution by direct methods (SHELXS) [7] produced a complete phasing model consistent with the proposed structure which was refined by least square methods on F^2 using the SHELXL-97 [7] program package. The refinement was continued until the maximum shift/e.s.d was 0.000. The final difference map was featureless with maximum and minimum electron densities at, respectively, 0.487 and $-0.630 \text{ e \AA}^{-3}$. The

Table 1 Crystal data and structure refinement for compound **1**

Empirical formula	C ₂₃ H ₃₃ N ₅ O ₄ Si
Formula weight	471.63
Temperature	173(2) K
Wavelength	1.54178 \AA
Crystal system	Monoclinic
Space group	$P2_1$
Unit cell dimensions	$a = 9.403(3) \text{ \AA}$, $\alpha = 90^\circ$ $b = 6.2828(12) \text{ \AA}$, $\beta = 96.505(16)^\circ$ $c = 20.681(5) \text{ \AA}$, $\gamma = 90^\circ$
Volume	1213.9(5) \AA^3
Z	2
Density (calculated)	1.290 Mg/m^3
Absorption coefficient	1.176 mm^{-1}
F(000)	504
Crystal size	$0.50 \times 0.10 \times 0.02 \text{ mm}^3$
Theta range for data collection	$4.30\text{--}63.78^\circ$
Index ranges	$(-10 \leq h \leq 10)$, $(-4 \leq k \leq 7)$, $(-23 \leq l \leq 23)$
Reflections collected	3691
Independent reflections	2578 [$R_{\text{int}} = 0.0675$]
Completeness to theta = 63.78°	90.8%
Absorption correction	Semi-empirical from equivalents
Max. and min. transmission	0.9769 and 0.5908
Refinement method	Full-matrix least-squares on F^2
Data/restraints/parameters	2578/1/305
Goodness-of-fit on F^2	1.103
Final R indices [$I > 2\sigma > (I)$]	$R_1 = 0.0961$, $wR_2 = 0.2448$
R indices (all data)	$R_1 = 0.1544$, $wR_2 = 0.3063$
Extinction coefficient	0.0064(19)
Largest diff. peak and hole	0.487 and $-0.630 \text{ e \AA}^{-3}$

crystal data, intensity collection conditions and refinement parameters are presented in Table 1. Atomic coordinates and equivalent isotropic displacement parameters are shown in Table 2. All non-hydrogen atoms were refined anisotropically (Table 3) by full-matrix least-squares. Selected bond lengths and bond angles are given in Tables 4 and 5. All H atoms were located geometrically, with C–H=0.95–1.0, N–H = 0.88 and O–H = 0.84 \AA and treated using a riding model, with isotropic U set to 1.2 or 1.5 times the isotropic equivalent of that of the attached parent atom. For the methyl group, the C–C–H angles and C–H distances were fixed, but the CH₃ group was allowed to rotate about the C–CH₃ bond.

Table 2 Atomic coordinates ($\times 10^4$) and equivalent isotropic displacement parameters ($\text{\AA}^2 \times 10^3$) for compound **1**

	x	y	z	U(eq)
Si(1)	4848(3)	5194(8)	1765(2)	43(1)
O(1)	−311(9)	13300(20)	2241(4)	55(3)
O(2)	−1088(8)	6654(18)	173(4)	45(3)
O(3)	3571(8)	9155(17)	226(4)	46(3)
N(5)	875(10)	6600(20)	−369(5)	37(3)
O(4)	3464(8)	6684(18)	1401(4)	48(3)
N(4)	524(10)	6690(20)	1388(4)	42(3)
N(3)	299(9)	10350(20)	1677(4)	44(3)
C(10)	−661(12)	9750(30)	2679(6)	55(5)
N(1)	−338(11)	5270(20)	4375(5)	46(3)
C(16)	3330(12)	6870(30)	217(6)	42(4)
C(14)	271(12)	6690(30)	188(6)	39(3)
C(12)	176(12)	8170(30)	1804(6)	44(4)
C(13)	1207(11)	7190(30)	808(5)	36(3)
C(15)	2434(12)	6210(30)	−395(5)	56(5)
N(2)	−290(10)	7760(20)	2365(5)	44(4)
C(22)	3455(15)	4360(30)	2878(7)	64(5)
C(20)	4767(14)	5530(30)	2682(6)	48(4)
C(11)	−205(12)	11320(30)	2185(6)	48(5)
C(1)	−1382(14)	6430(30)	4586(6)	45(4)
C(2)	−2266(15)	6080(30)	5065(6)	60(5)
C(5)	−2363(14)	9980(40)	4375(6)	64(5)
C(18)	6555(13)	6330(30)	1519(6)	48(4)
C(6)	−1374(13)	8430(20)	4248(6)	40(3)
C(7)	−271(14)	8280(30)	3831(6)	51(4)
C(21)	6125(13)	4580(30)	3065(6)	61(5)
C(3)	−3198(16)	7690(40)	5189(7)	67(6)
C(8)	349(14)	6320(30)	3919(6)	57(5)
C(4)	−3260(15)	9640(30)	4846(8)	67(6)
C(17)	2658(12)	6120(30)	811(6)	55(5)
C(23)	4666(18)	7920(40)	2848(8)	86(7)
C(9)	138(14)	10010(30)	3352(5)	51(4)
C(19)	4643(15)	2310(30)	1538(7)	53(4)

U(eq) is defined as one third of the trace of the orthogonalized U^{ij} tensor

Table 3 Anisotropic displacement parameters ($\text{\AA}^2 \times 10^3$) for compound **1**

	U^{11}	U^{22}	U^{33}	U^{23}	U^{13}	U^{12}
Si(1)	29(2)	56(3)	44(2)	0(2)	0(1)	-2(2)
O(1)	48(5)	70(11)	49(5)	-4(6)	12(4)	17(6)
O(2)	35(4)	46(8)	53(5)	-3(5)	-3(4)	-1(5)
O(3)	28(4)	64(9)	46(5)	-3(5)	9(4)	-1(5)
N(5)	33(5)	31(8)	47(5)	4(5)	2(4)	-2(5)
O(4)	32(4)	63(8)	46(4)	-7(5)	-10(4)	10(5)
N(4)	34(5)	56(10)	40(5)	4(6)	17(4)	3(6)
N(3)	35(5)	64(10)	33(5)	18(6)	6(4)	-1(7)
C(10)	33(6)	91(16)	43(7)	-12(9)	12(5)	11(8)
N(1)	56(6)	31(8)	52(6)	3(6)	8(5)	0(8)
C(16)	30(6)	42(12)	54(7)	-2(7)	7(5)	-14(7)
C(14)	28(6)	38(11)	51(7)	2(7)	-1(5)	2(7)
C(12)	22(6)	73(15)	37(6)	1(8)	6(5)	-2(7)
C(13)	30(6)	36(10)	42(6)	0(6)	3(5)	2(6)
C(15)	32(6)	105(17)	33(6)	-10(7)	11(5)	13(8)
N(2)	30(5)	67(12)	35(5)	-8(6)	9(4)	-2(6)
C(22)	55(8)	85(16)	57(8)	11(9)	25(7)	10(9)
C(20)	49(7)	48(13)	48(6)	4(8)	12(6)	5(9)
C(11)	27(6)	82(17)	37(7)	-11(8)	9(5)	17(8)
C(1)	46(7)	31(11)	57(8)	3(7)	-5(6)	-6(8)
C(2)	55(8)	77(16)	50(8)	-6(8)	9(7)	-14(9)
C(5)	52(8)	86(16)	50(7)	-4(9)	-13(6)	19(11)
C(18)	37(6)	47(12)	58(7)	-14(7)	4(6)	-17(7)
C(6)	38(6)	22(10)	58(8)	0(7)	-4(6)	0(7)
C(7)	49(8)	66(14)	38(6)	-8(7)	2(6)	-5(9)
C(21)	44(7)	84(16)	50(7)	-11(8)	-11(6)	5(9)
C(3)	42(8)	100(20)	59(9)	-12(10)	13(7)	-19(10)
C(8)	37(7)	87(17)	45(7)	-17(8)	3(6)	12(8)
C(4)	45(8)	77(18)	76(10)	-18(10)	-2(7)	-3(10)
C(17)	27(6)	95(17)	43(7)	4(7)	4(5)	4(7)
C(23)	69(11)	120(20)	68(10)	-2(12)	4(8)	8(13)
C(9)	60(7)	57(12)	37(6)	11(8)	5(6)	-14(9)
C(19)	52(8)	23(11)	81(9)	-8(8)	-9(7)	9(8)

The anisotropic displacement factor exponent has the form $-2\pi^2[h^2 a^{*2}U^{11} + \dots + 2hk a^* b^* U^{12}]$

Results and Discussion

As outlined in the introduction, hydrogenolysis of **5** to remove the Cbz group furnished the highly substituted imidazolinone **1** as a major product and not the expected deprotected scaffold (Fig. 2). Even under the mild conditions of the hydrogenation, intramolecular nucleophilic attack of the α -amino group at the electrophilic carbon center of the oxazoline **6** was favored, leading to the formation of **1** instead. This conversion might be exploited to obtain 2,5-disubstituted imidazolin-4-ones from condensation of

Table 4 Selected bond lengths [\AA] for compound **1**

Si(1)–O(4)	1.707(9)
O(1)–C(11)	1.25(2)
O(2)–C(14)	1.275(14)
O(3)–C(16)	1.456(19)
N(5)–C(14)	1.343(15)
N(5)–C(15)	1.494(15)
O(4)–C(17)	1.408(14)
N(4)–C(12)	1.329(19)
N(4)–C(13)	1.458(14)
N(3)–C(11)	1.345(17)
N(3)–C(12)	1.40(2)
C(10)–N(2)	1.47(2)
C(10)–C(9)	1.515(16)
C(10)–C(11)	1.52(2)
N(1)–C(1)	1.336(18)
N(1)–C(8)	1.369(19)
C(16)–C(15)	1.496(17)
C(16)–C(17)	1.517(18)
C(14)–C(13)	1.503(15)
C(12)–N(2)	1.311(15)
C(13)–C(17)	1.521(16)
C(1)–C(2)	1.380(19)
C(1)–C(6)	1.44(2)
C(2)–C(3)	1.38(2)
C(5)–C(4)	1.38(2)
C(5)–C(6)	1.39(2)
C(6)–C(7)	1.426(19)
C(7)–C(8)	1.37(2)
C(7)–C(9)	1.55(2)
C(3)–C(4)	1.41(3)

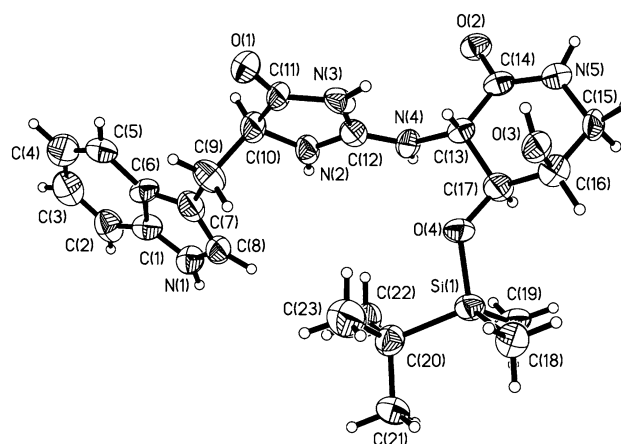
amino-oxazoline lactam (**3**) with a variety of Cbz-protected α -amino acids followed by hydrogenolysis.

Crystal Structure

Compound **1** crystallized in the monoclinic $P2_1$ space group with two molecules in the unit cell. An ORTEP drawing of the molecule with atom numbering scheme is shown in Fig. 3. The six- and five-membered rings which consist of the C1–C6–C7–C8–N1 and C1–C2–C3–C4–C5–C6 atoms are nearly co-planar with a dihedral angle of 2.8° between the two mean planes. The C13–C14–N5–C15–C16–C17 six-membered ring adopts a distorted chair-like conformation with the C13–C17–C16 and C14–N5–C15 planes oriented at 54.2° and 21.5° to the main C13–C14–C15–C16 plane (mean deviation from plane = 0.0248 \AA). The bulky OTBDMS group is in the equatorial position on this six-membered ring. The N2–C12 and N4–C12 bond lengths in the molecule (1.311(15) and 1.329(19) \AA ,

Table 5 Selected bond angles [°] for compound **1**

C(14)–N(5)–C(15)	123.3(9)
C(17)–O(4)–Si(1)	123.6(10)
C(12)–N(4)–C(13)	123.1(13)
C(11)–N(3)–C(12)	104.7(13)
N(2)–C(10)–C(9)	112.4(13)
N(2)–C(10)–C(11)	99.0(10)
C(9)–C(10)–C(11)	113.6(12)
C(1)–N(1)–C(8)	112.7(15)
O(3)–C(16)–C(15)	110.8(13)
O(3)–C(16)–C(17)	112.0(12)
C(15)–C(16)–C(17)	110.6(11)
O(2)–C(14)–N(5)	119.9(9)
O(2)–C(14)–C(13)	120.9(11)
N(5)–C(14)–C(13)	118.4(9)
N(2)–C(12)–N(4)	124.7(17)
N(2)–C(12)–N(3)	113.4(14)
N(4)–C(12)–N(3)	121.9(12)
N(4)–C(13)–C(14)	112.7(10)
N(4)–C(13)–C(17)	112.3(10)
C(14)–C(13)–C(17)	110.4(10)
N(5)–C(15)–C(16)	112.7(10)
C(12)–N(2)–C(10)	110.3(14)
C(22)–C(20)–C(23)	109.8(14)
C(22)–C(20)–C(21)	108.8(14)
C(23)–C(20)–C(21)	109.3(13)
C(22)–C(20)–Si(1)	109.3(10)
C(23)–C(20)–Si(1)	109.7(11)
C(21)–C(20)–Si(1)	109.9(9)
O(1)–C(11)–N(3)	124.1(15)
O(1)–C(11)–C(10)	123.4(12)
N(3)–C(11)–C(10)	112.5(17)
N(1)–C(1)–C(2)	132.1(16)
N(1)–C(1)–C(6)	105.9(12)
C(2)–C(1)–C(6)	121.8(15)
C(1)–C(2)–C(3)	117.4(16)
C(4)–C(5)–C(6)	120.1(18)
C(5)–C(6)–C(7)	135.4(16)
C(5)–C(6)–C(1)	118.5(14)
C(7)–C(6)–C(1)	106.1(13)
C(8)–C(7)–C(6)	108.1(14)
C(8)–C(7)–C(9)	125.9(14)
C(6)–C(7)–C(9)	125.9(15)
C(2)–C(3)–C(4)	122.2(15)
C(7)–C(8)–N(1)	107.2(13)
C(5)–C(4)–C(3)	119.8(17)
O(4)–C(17)–C(16)	113.0(11)
O(4)–C(17)–C(13)	106.6(11)
C(16)–C(17)–C(13)	108.3(11)
C(10)–C(9)–C(7)	112.2(12)

**Fig. 3** ORTEP plot of compound **1**. Thermal ellipsoids are shown at 50% probability**Table 6** Hydrogen bond lengths [Å] and angles [°] for compound **1**

D–H...A	<i>d</i> (D–H)	<i>d</i> (H...A)	<i>d</i> (D...A)	∠(DHA)
O(3)–H(3)...O(2)#1	0.84	2.02	2.856(13)	172.5
N(4)–H(4)...O(1)#2	0.88	2.20	2.932(17)	140.9
N(2)–H(2)...O(1)#2	0.88	2.09	2.815(19)	139.3

Symmetry transformations used to generate equivalent atoms

#1 $-x, y + 1/2, -z$; #2 $x, y - 1, z$

respectively) are significantly shorter than the 1.472–1479 Å range for an ideal C–N single bond [8]. This indicates a significant π -charge delocalization along the N2–C12–N4 moiety. To reflect this fact in the crystal structure, corresponding hydrogen atoms were assigned at 50% occupancy. The N3–C11 bond distance of 1.345(17) Å is in agreement with the N5–C14 bond of the six-membered ring with its length of 1.343(15) Å. Shortening of these bonds with respect to the ideal single C–N bond originates from the neighboring carbonyl moieties. The N3–C12 bond of 1.40(2) Å is also shorter than the ideal C–N single bond indicating the influence of the delocalized N2–C12–N4 region on this bond. The C10–C11 and C10–N2 bond lengths are normal with 1.52(2) and 1.47(2) Å, respectively. The crystal packing of **1** is achieved through a complex network of hydrogen bonds (Table 6) occurring between neighboring molecules. Intermolecular hydrogen bonding is observed between N2–H2...O1 [N2...O1 = 2.815(19) Å, O1...H2 = 2.09 Å] and between N4–H4...O1 [N4...O1 = 2.932(17) Å, O1...H4 = 2.20 Å], which form between two molecules in the crystal lattice. These intermolecular interactions result in the formation of molecular chains. The adjacent chains further interact with each other in the lattice structure through an O3–H3...O2 hydrogen bond [O3...O2 = 2.856(13) Å,

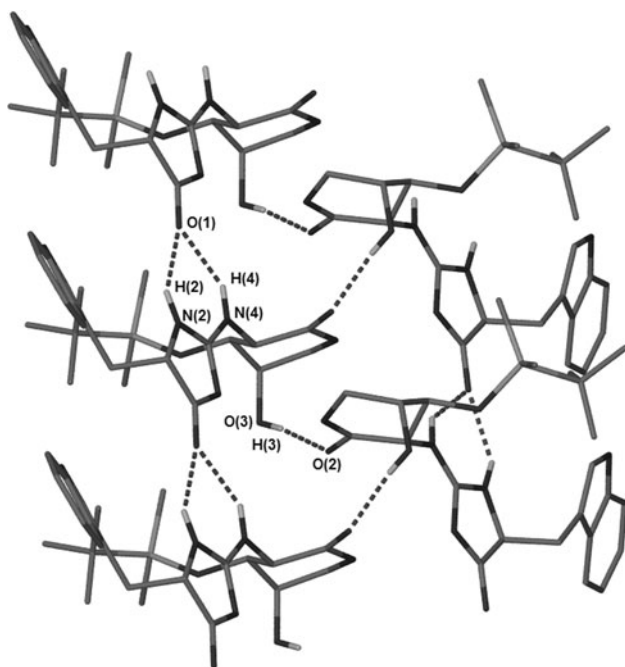


Fig. 4 Intermolecular hydrogen bonding pattern in the crystal of **1**. Hydrogen bonds are shown as *dashed lines*. The hydrogen atoms involved in the hydrogen-bonding network are shown, while the others are omitted for clarity

$O2 \cdots H3 = 2.02 \text{ \AA}$]. These hydrogen bonding interactions lead to the formation of the dimeric chain structure in the lattice as shown in the Fig. 4.

Supplementary Material

CCDC 811834 contains the supplementary crystallographic data for this paper. These data can be obtained free of charge by e-mailing data_request@ccdc.cam.ac.uk, or by contacting The Cambridge Crystallographic Data Centre, 12 Union Road, Cambridge CB2 1EZ, UK, Fax: +44(0)1223-336033.

Acknowledgments This work was supported in part by the National Institutes of Health, Grant Nos. AI72012 and CA132753. Support of the NMR facility by the National Science Foundation is acknowledged (CRIF grant CHE-0741968).

References

- Haupt I, Hübener R, Thrum H (1978) *J Antibiot* 31:1137
- Jackson MD, Gould SJ, Zabriskie TM (2002) *J Org Chem* 67:2934
- Gant TG, Meyers AI (1994) *Tetrahedron* 50:2297
- Dutta S, Higginson CJ, Ho BT, Rynearson KD, Dibrov SM, Hermann T (2010) *Org Lett* 12:360
- Bruker SAINT (2005) Bruker AXS Inc. Madison, WI
- Bruker AXS (2001) SADABS: v.2.01, an empirical absorption correction program. Bruker AXS, Madison
- Sheldrick GM (1997) SHELX-97, program for crystal structure refinement. University of Gottingen, Germany
- Uppsala Software Factory (1997) Typical bond lengths. http://hmi.swmed.edu/Manuals/gerard/typical_bonds.html